One Earth

Article

Warming of northern peatlands increases the global temperature overshoot challenge

Graphical abstract

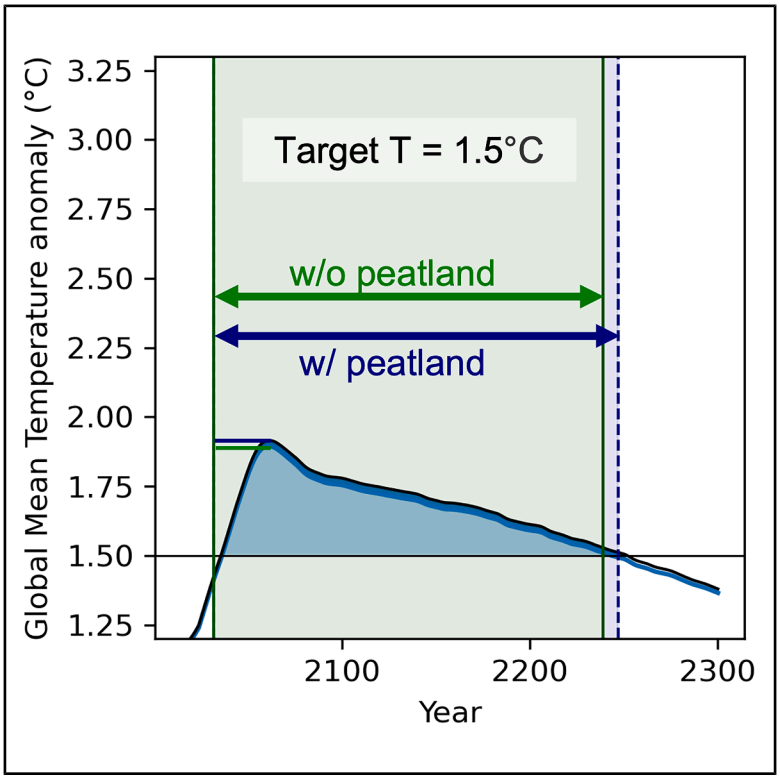

Highlights

- Peatlands amplify climate feedbacks under 1.5°C–2.5°C overshoot scenarios
- Methane drives peatlands' net positive feedback despite higher carbon uptake
- Peatlands reduce the carbon budget by 37 $GtCO_2$ per 1°C of global temperature change
- Peatlands increase carbon removal needs by 40 $GtCO_2$ if the 1.5°C target is overshot

Authors

Biqing Zhu, Chunjing Qiu, Thomas Gasser, ..., Wenxin Zhang, Yuan Zhang, Dan Zhu

Correspondence

zhub@iiasa.ac.at (B.Z.), cjqiu@des.ecnu.edu.cn (C.Q.)

In brief

The study highlights the critical role of northern peatlands in amplifying climate change under overshoot scenarios, that is, when global temperature temporarily exceeds the targeted level. We simulate that in such scenarios the peatland carbon uptake is offset by increased methane emissions, which amplifies and lengthens the overshoot and reduces the anthropogenic emissions compatible with a given warming level. Our findings emphasize the importance of accounting for peatland dynamics in climate models, especially in overshoot pathways.

Zhu et al., 2025, One Earth *8*, 101353
August 15, 2025
https://doi.org/10.1016/j.oneear.2025.101353

One Earth

CellPress
OPEN ACCESS

Article

Warming of northern peatlands increases the global temperature overshoot challenge

Biqing Zhu,[1,2,29,30,*] Chunjing Qiu,[2,3,4,29,*] Thomas Gasser,[1,2] Philippe Ciais,[2] Robin D. Lamboll,[5] Ashley Ballantyne,[2,6] Jinfeng Chang,[7] Nitin Chaudhary,[8,9,10] Angela V. Gallego-Sala,[11] Bertrand Guenet,[12] Joseph Holden,[13] Fortunat Joos,[14,15] Thomas Kleinen,[16] Min Jung Kwon,[2,17] Irina Melnikova,[2,18] Jurek Müller,[14,15] Susan Page,[19] Elodie Salmon,[2] Carl-Friedrich Schleussner,[1,20,21] Guy Schurgers,[22] Gaurav P. Shrivastav,[1] Narasinha J. Shurpali,[23] Katsumasa Tanaka,[2,18] David Wårlind,[8] Sebastian Westermann,[24,28] Yi Xi,[2] Wenxin Zhang,[8,25] Yuan Zhang,[26] and Dan Zhu[27]

[1]International Institute for Applied Systems Analysis (IIASA), 2361 Laxenburg, Austria
[2]Laboratoire des Sciences du Climat et de l'Environnement (LSCE), CEA–CNRS– UVSQ, IPSL, Université Paris-Saclay, 91191 Gif-sur-Yvette, France
[3]Research Center for Global Change and Ecological Forecasting, School of Ecological and Environmental Sciences, East China Normal University, Shanghai, China
[4]Institute of Eco-Chongming, East China Normal University, Shanghai, China

(Affiliations continued on next page)

SCIENCE FOR SOCIETY Northern peatlands store vast amounts of carbon. These ecosystems are warming faster than the global average, threatening to release more carbon into the atmosphere and accelerate climate change. Understanding how peatlands react to warming and how they might feedback into climate change is a pressing challenge. Current climate models often overlook the complex behavior of peatlands, leaving significant uncertainties in predictions.

Our study fills this gap by evaluating the impact of northern peatlands on global climate projections, particularly under scenarios where the 1.5°C temperature target is temporarily overshot. We find that peatlands could increase carbon removal requirements by up to 8.6% if this target is exceeded, underscoring their importance in climate mitigation efforts. This research highlights the need to better incorporate peatlands into climate models to improve future policy decisions and more accurately assess the path to meeting climate goals.

SUMMARY

Meeting the Paris Agreement's temperature goals requires limiting future carbon emissions, yet current policies make temporarily overshooting the 1.5°C target likely. The potential climate feedback from destabilizing peatlands, storing large amounts of carbon, remains poorly quantified. Using the reduced-complexity Earth System Model OSCAR with an integrated peat carbon module, we found that across various overshoot pathways that temporarily exceed 1.5°C–2.5°C, northern peatlands exhibit net positive feedback, amplifying the overshoot challenge. Warming increases peatlands' net carbon uptake, but this is largely offset by higher methane emissions. We estimated that for each 1°C increase in peak warming, the positive feedback from peatlands decreases the remaining carbon budget by 37 $GtCO_2$ (22–48 $GtCO_2$). If the 1.5°C temperature target is exceeded, peatlands would increase carbon removal requirement by about 40 $GtCO_2$ (16–60 $GtCO_2$) (8.6%). Our findings highlight the importance of properly accounting for northern peatlands for estimating climate feedbacks, especially under overshoot scenarios.

INTRODUCTION

Northern peatlands (>30°N) store 400–600 Pg C in soils, and are projected to undergo more pronounced warming than the global average.[1,2] If part of this carbon is destabilized, it could potentially cause large amplifying feedback on climate warming. The direction and strength of peatland feedbacks are determined by the sensitivity of peatland CO_2 and CH_4 fluxes to climate change. Peat vegetation productivity can increase with warming and rising atmospheric CO_2 levels, representing an increased

[5]Centre for Environmental Policy, Imperial College London, London, UK
[6]Department of Ecosystem and Conservation Science, University of Montana, Missoula, MT 59801, USA
[7]College of Environmental and Resource Sciences, Zhejiang University, Hangzhou, China
[8]Department of Physical Geography and Ecosystem Science, Lund University, 22362 Lund, Sweden
[9]Centre for Environmental and Climate Science (CEC), Lund University, 22362 Lund, Sweden
[10]Stockholm Resilience Centre, Stockholm University, Stockholm, Sweden
[11]Geography Department, Faculty of Environment, Science and Economy, University of Exeter, Exeter EX4 4RJ, UK
[12]LG-ENS (Laboratoire de Géologie) CNRS UMR 8538 - Ecole Normale Supérieure, PSL University - IPSL, Paris, France
[13]School of Geography, University of Leeds, Leeds LS2 9JT, UK
[14]Climate and Environmental Physics, Physics Institute, University of Bern, 3012 Bern, Switzerland
[15]Oeschger Center for Climate Change Research, University of Bern, 3012 Bern, Switzerland
[16]Max Planck Institute for Meteorology, 20146 Hamburg, Germany
[17]Institute of Soil Science, University of Hamburg, Hamburg, Germany
[18]Earth System Division, National Institute for Environmental Studies (NIES), Tsukuba, Japan
[19]School of Geography, Geology and the Environment, University of Leicester, Leicester, UK
[20]Climate Analytics, Berlin, Germany
[21]Geography Department and IRITHESys Institute, Humboldt-Universität zu Berlin, Berlin, Germany
[22]Department of Geosciences and Natural Resource Management, University of Copenhagen, Copenhagen, Denmark
[23]Natural Resources Institute Finland, Production Systems, Halolantie 31 A, 71750 Maaninka, Finland
[24]Department of Geosciences, University of Oslo, 0371 Oslo, Norway
[25]School of Geographical and Earth Sciences, University of Glasgow, Glasgow G12 8QQ, UK
[26]State Key Laboratory of Tibetan Plateau Earth System, Environment and Resources (TPESER), Institute of Tibetan Plateau Research, Chinese Academy of Sciences, Beijing, China
[27]Sino-French Institute for Earth System Science, College of Urban and Environmental Sciences, Peking University, Beijing, China
[28]Centre for Biogeochemistry in the Anthropocene, University of Oslo, Norway
[29]These authors contributed equally
[30]Lead contact
*Correspondence: zhub@iiasa.ac.at (B.Z.), cjqiu@des.ecnu.edu.cn (C.Q.)
https://doi.org/10.1016/j.oneear.2025.101353

carbon sink, but warming can also accelerate peat carbon decomposition and could turn these ecosystems into net CO_2 sources.[3,4] Meanwhile, peatland methane (CH_4) emissions could increase in response to warming if the ecosystem remains wet.[5]

Only a few process-based land surface models have included peatland biogeochemistry dynamics. Peatlands are also not explicitly represented in the current generation of Earth system models (ESMs). Consequently, efforts to quantify the peatland carbon-climate feedback are limited. Qiu et al. (2020),[3] however, estimated that CO_2 removal by northern peatland will roughly double from the mean annual balance of 0.10 PgC/year over 1861–2005, by the end of the century under both RCP2.6 and RCP6.0.[6] Under the RCP8.5 scenario, they predicted that northern peatlands will become either carbon-neutral or a source of CO_2 by the end of the 21st century, depending on the climate forcing used to drive the model. Müller and Joos (2021),[4] in seamless simulations from the last glacial maximum to the next 5,000 years, predicted future net losses in global peatland area and carbon, with greater losses expected under higher emission scenarios. In addition, substantial uncertainty in projected peatland changes was found due to climate forcing, with committed historical changes and future rising temperature as the main driver of future peatland loss and increasing precipitations as the driver for regional peatland expansion. Chaudhary et al. (2022)[7] used a peatland-vegetation model (LPJ-GUESS) that includes dynamic peat accumulation and decomposition functionalities with representation of freeze-thaw processes. Peatlands are projected to remain carbon sink under the RCP2.6 to RCP6.0 scenarios, but will shift from a carbon sink to a carbon neutral in RCP8.5.[7] A recent study incorporating five advanced process-based land surface models, with consistent climate forcing across models, projected that northern peatlands will remain climate neutral under RCP2.6.[3] However, under RCP8.5, they are expected to release both CO_2 and CH_4 over the long term, contributing an additional warming of 0.21°C (+0.09°C to +0.49°C).[3] The significant uncertainties in the estimated peatland carbon-climate feedback arise not only from the varying representations of peatland biogeochemical processes across different models but also from the choice of climate forcing and model initialization. Despite previous research highlighting these uncertainties, the issue remains insufficiently studied.[3,4]

These substantial uncertainties in peatland carbon-climate feedback lead to divergent projections regarding the future role of northern peatlands and are critical to address for effective climate mitigation efforts. However, integrating peatlands into complex ESMs to explore the uncertainty remains challenging, as these require extensive computational resources to run, often ranging from days to months for a single simulation. When evaluating climate mitigation scenarios, it is essential to explore a broad range of scenarios,[6] which further exacerbates the impracticality of the approach. As an alternative, reduced-complexity ESMs and ESMs of intermediate complexity offer valuable advantages. They are computationally efficient and particularly effective for investigating couplings and uncertainties, allowing for the exploration of large ensembles of scenarios and for statistical analyses of uncertainties in model parameters.[8–10]

Previous efforts to quantify the peatland carbon-climate feedback have primarily focused on business-as-usual scenarios that exceed the Paris climate targets and strong climate mitigation scenarios that align with the targets,[3,11] and they have relied on offline land-only models.[3,4] There is a lack of

studies investigating the topic in the context of overshooting climate targets. Although the Paris Agreement has set the goal to pursue efforts to limit global surface air temperature (GSAT) increase to 1.5°C above pre-industrial levels, under current climate policies it seems increasingly unlikely that such a target will be achieved without temporary exceedance (overshoot). Carbon emissions from northern peatlands triggered by climate change may increase the chance of overshoot, the intensity of it, and/or its duration. This potential amplifying feedback from northern peatlands will make it more difficult to return to the target temperature, requiring notably more anthropogenic carbon removal.

Here we investigate the critical role of northern peatlands in climate change mitigation by systematically evaluating their impact on peak temperature, overshoot duration, and the global carbon budget. This work addresses an important gap in current Earth system modeling, where peatland dynamics are underrepresented, contributing to significant uncertainty in future climate projections and mitigation planning. By applying the reduced-complexity ESM OSCAR v3.1.2 enhanced with a newly integrated peat carbon module, we simulate a wide range of emission scenarios, with a focus on overshoot. We find that accounting for peatlands feedback would result in an additional 8.6% increase in carbon capture needed if the 1.5°C temperature target is overshot, with better-case estimates of 5.2% and worse-case estimates of up to 68% to return below the 1.5°C threshold. These findings highlight the substantial influence of peatlands on future mitigation pathways and demonstrate the importance of accounting for peatlands in climate policy assessments. Overall, this study provides a systematic evaluation of peatland-driven feedback and advances understanding of their implications for meeting climate mitigation targets.

RESULTS

Methods summary

To quantify the role of northern peatland in climate change mitigation, we use the reduced-complexity ESM OSCAR3.2.1, enhanced with a newly developed peat carbon module. This peat module emulates peatland processes from five state-of-the-art process-based land surface models: LPJ-MPI,[12] ORCHIDEE-PEAT,[8,9] LPX-Bern,[4,10,11,13] LPJ-GUESS,[14,15] and LPJ-GUESS_dynP (dynP for dynamic multi-peat layers).[11,16,17] Each of these simulates the complex peat ecosystem differently, incorporating distinct approaches to representing peat hydrology, biogeochemistry, vegetation, and soil thermal dynamics, which are critical drivers of feedback uncertainty. These various representations of peatland processes in the land surface models are implicitly incorporated by the emulator. A detailed description of the complex peat models is provided as Note S1, while that of the peat-emulating module is in the methods.

We investigate a wide range of scenarios that keep the GSAT anomaly below levels of 1.5°C, 2°C, or 2.5°C by 2300. In total, 282 emission pathways crafted for the PROVIDE project (hereafter called "PROVIDE scenarios")[18] and eight shared socio-economic pathway (SSP) scenarios[19–21] are used to drive OSCAR (Figure 1A). To assess the impact of peatland dynamics on future warming and atmospheric CO_2 and CH_4 levels, we ran OSCAR under two setups: one with the peat module activated and one without, representing the Earth system with and without perturbation of peat carbon. The additional feedback caused by northern peatlands is derived as the difference between both experiments.

We investigate the critical role of northern peatlands in climate change mitigation by systematically evaluating their impact on peak temperature, overshoot duration, and the global carbon budget. The latter has two aspects: the remaining carbon budget that describes the amount of cumulative anthropogenic CO_2 emissions that can still be emitted while keeping global temperature below a given warming target, and the carbon removal requirements that describe the carbon capture needed to return global temperature to a target level after overshooting it. Furthermore, we quantify uncertainties from inter-model differences in peatland representation, climate projections, and scenarios. Our approach offers unique insights into these uncertainties and provides valuable insights for informing climate mitigation strategies. More details regarding the protocol are provided in the methods.

Projected warming and peatland emissions

With the peat carbon module turned off, the simulated GSAT anomaly in 2100 with respect to pre-industrial is 1.3°C (1.0°C – 1.6°C) in the low-emission SSP1-1.9 scenario and 3.9°C (3.1°C –4.7°C) in the high-emission SSP5-8.5 (uncertainty ranges in brackets denote the 68% confidence interval [CI]; see methods). By 2300, the GSAT anomaly is projected to range from 0.7°C (0.4°C –0.9°C) to 6.4°C (5.0°C –7.8°C) (Figure 1C). For global warming levels of 1.5°C, 2°C, and 2.5°C, we analyze overshoot scenarios in which the GSAT anomaly temporarily exceeds that level but falls back below by 2300. The overshoot scenarios, exemplified by the SSP5-3.4-OS scenario in Figure 1C, are characterized by their peak temperature anomaly (Tpeak), and the year this peak is reached (YRpeak).

Across all scenarios, Tpeak ranged from 1.5°C (1.3°C –1.8°C) to 6.4°C (5.0°C –7.8°C). The overshoot duration ranged from 7 to 262 years, with median values of 165, 107, and 102 years for global warming levels of 1.5°C, 2°C, and 2.5°C, respectively (uncertainty inapplicable for overshoot duration, thus not reported, Table S1). Without the additional feedback of northern peatlands, the projected peak atmospheric CO_2 concentration anomaly ranged from 149 ppm (131–168 ppm) in the most optimistic scenario, to 981 ppm (812–1,143 ppm) ppm in the most pessimistic scenario (Figure 1B).

In our simulations, the change in northern peatland CH_4 emissions follows a trajectory similar to that of GSAT, while the northern peatland CO_2 sink is projected to increase from 0.04 PgC y^{-1} (0–0.13 PgC y^{-1}) to 0.06 PgC y^{-1} (0–0.23 PgC y^{-1}) (relative to pre-industrial) before decreasing across scenarios (Figures 1D and 1E). The turning year at which the time derivative of the peat CO_2 sinks changes sign from positive to negative is different across scenarios, ranging from year 2022 to year 2056. GSAT in 2100 is 0.02°C (0.01–0.04°C) to 0.04°C (0.02–0.06°C) warmer when considering both CO_2 and CH_4 fluxes from peatlands than without considering peatlands (Figure 1F). In 2300, the impact of peatlands on GSAT ranged from 0.00°C (0.00–0.10°C) to 0.09°C (0.02–0.10°C) across scenarios.

Amplification of warming by peatland CH_4 emissions

While in our simulations the rate of northern peatland CH_4 emissions increases seemingly linearly with GSAT (at about 3.8 TgC

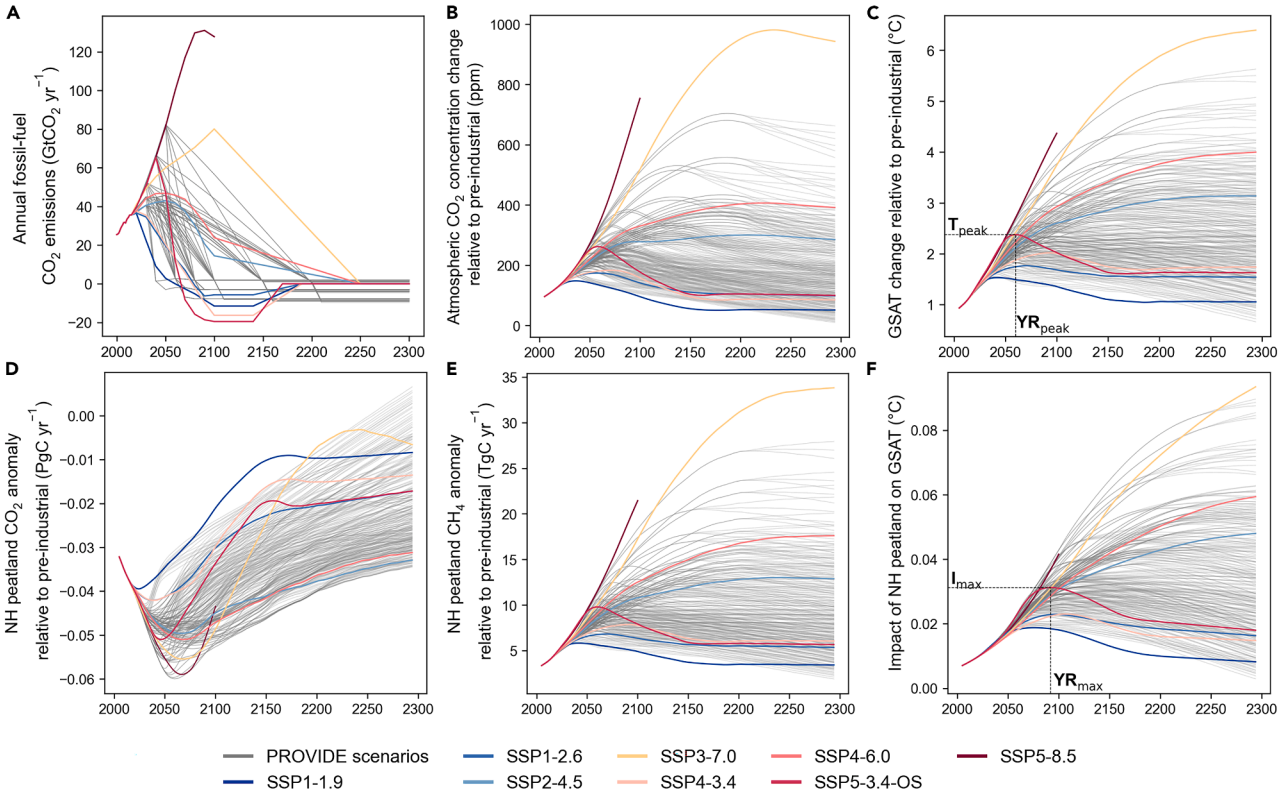

Figure 1. Emissions, climate and carbon responses under various scenarios

The colored lines represent SSPs. The gray lines indicate the PROVIDE scenarios, which are a set of 282 emission pathways with a focus on overshoot (202 of which exceed 1.5°C, 2°C, and 2.5°C global warming level before returning below).

(A) Annual fossil fuel CO_2 emissions.

(B) Corresponding atmospheric CO_2 concentration anomaly.

(C) GSAT anomaly with the peat module turned off.

(D) Peatland CO_2 flux anomaly, negative values indicating a stronger sink compared to pre-industrial and zero values a transition to a CO_2 source anomaly.

(E) Northern peatland CH_4 emission anomaly.

(F) Impact of northern peatlands on GSAT, calculated as the difference between the simulation with peatlands minus the simulation without peatlands. The total GSAT anomaly with peatland feedback is the sum of the curves in (C) and (F) (SSP5-8.5 stops in 2100 for readability). Peak temperature anomaly is noted as Tpeak. The year this peak is reached is noted as YRpeak.

All values displayed are the best-guess values only, details described in the methods.

y^{-1} per °C of warming), the peatland CO_2 sink is controlled by both temperature and atmospheric CO_2 concentrations (Figures 2A and 2B). The peatland CO_2 sink first increases with GSAT and then decreases, but the turning point is also controlled by the atmospheric CO_2 concentrations because of the CO_2 fertilization effect on plant photosynthesis. For instance, under the SSP2-4.5 scenario, the trend of the northern peatland CO_2 sinks reverses (from increasing CO_2 sink to decreasing CO_2 sink) when the GSAT anomaly relative to pre-industrial reaches 2.2°C and the atmospheric CO_2 anomaly is 250 ppm above pre-industrial conditions. In contrast, under the SSP5-8.5 scenario, the trend reverses when the GSAT anomaly reaches 3.0°C and the atmospheric CO_2 anomaly is 404 ppm.

Because the warming effect caused by peatland CH_4 emissions exceeds the cooling effect from the peatland CO_2 sink, northern peatlands constitute positive feedback on global warming (Figure 2C). Across the various scenarios, the range of the feedback widens with increasing levels of warming, primarily because of the greater range of atmospheric CO_2 concentrations among scenarios with higher levels of warming. For instance, the atmospheric CO_2 concentration is projected to increase by 181–256 ppm depending on scenarios when the GSAT increases by 2°C, while it increases by 387–645 ppm when the GSAT increases by 4°C. Notably, for a given warming level, northern peatlands have smaller positive feedback under a higher emission pathway scenario than under a lower emission scenario, owing to a greater cooling effect from the peatland CO_2 sink (Figure 2C).

Peatland carbon release under overshoot scenarios

We assessed the peatland carbon storage change (ΔC, computed as the negative cumulative sum of carbon in peatland CO_2 and CH_4 fluxes) during the temperature overshoot. Despite a positive warming feedback (Figure 2C), peatlands exhibit a net carbon gain (Figure 3A), indicating that while peatlands accumulate carbon, they contribute to the Earth system's warming

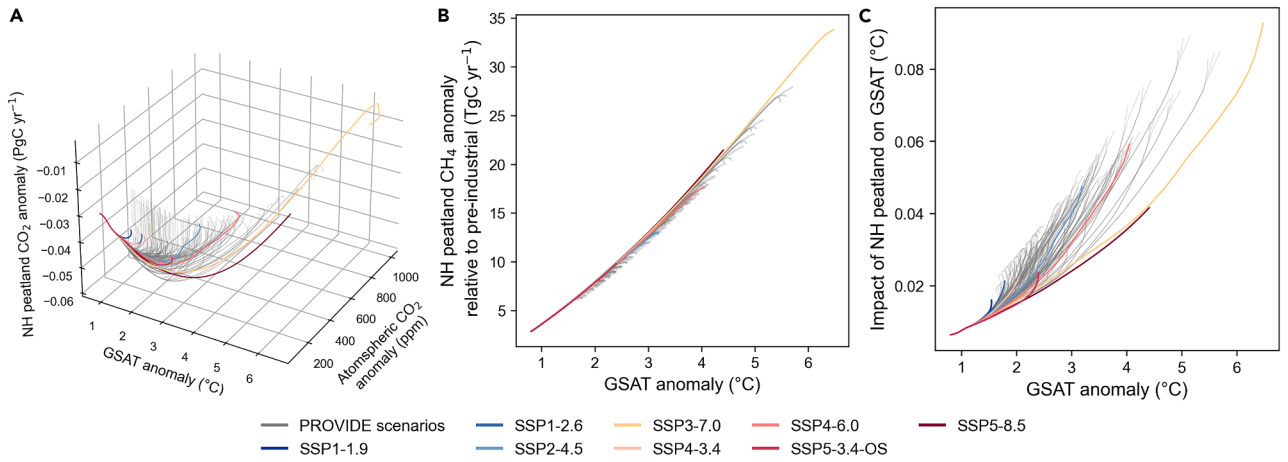

Figure 2. Northern peatland carbon dioxide (CO_2), methane (CH_4), and temperature feedback

The colored lines represent SSPs. The gray lines indicate the PROVIDE scenarios, which are a set of 282 emission pathways with a focus on overshoot (202 of which exceed 1.5°C, 2°C, and 2.5°C global warming level before returning below).

(A) Northern peatland CO_2 anomaly.

(B) Northern peatland CH_4 anomaly.

(C) Impact of northern peatland on GSAT (with peatland minus without peatland) as a function of GSAT anomaly.

through their high CH_4 emissions (Figure 3E). The ΔC between 2000 and 2300 ranges from 23 PgC gains (13–43 PgC gains) to 35 PgC gains (11–78 PgC gains), and shows slight positive correlation with Tpeak (Figure 3A). The cumulative CO_2 fluxes from peatland over the same period shows a slight negative correlation with Tpeak (Figure 3C) and ranges from −42 PgC (−84 to 19 PgC) to −34 PgC (−52 to 5 PgC). The corresponding cumulative CH_4 emissions positively correlates with Tpeak (Figure 3E) and ranges from 6.9 PgC (5.8–7.8 PgC) to 11.7 PgC (8.1–17.8 PgC). With a 1°C increase in Tpeak, northern peatlands ΔC increases by 2.5 PgC (0.1–12.7 PgC) (Figure 3A), CO_2 fluxes from peatlands decrease by 3.8 PgC (2.5–13.6 PgC), and CH_4 emissions increase by 1.2 PgC (0.9–2.5 PgC) respectively (Figure 3C).

Another way to analyze the greenhouse gas response of northern peatlands is to consider the integrated overshoot temperature over time (cumulative overshoot temperature in Figures 3B, 3D, and 3F). Here, we found that ΔC and CO_2 fluxes from peatlands do not show any correlation to the cumulative overshoot temperature (Figure 3B), whereas cumulative CH_4 emissions show significant and positive correlation with cumulative overshoot temperature (Figure 3F).

It is noteworthy that the uncertainty bars in Figure 3 account for uncertainties from different peatland representations, as well as from all other earth system processes included in OSCAR. Significant differences exist in how peatland vegetation, peat carbon pools, carbon fluxes, and peatland soil thermal and hydraulic processes are represented by the complex peatland-resolving models used to calibrate OSCAR. These differences are highlighted by simulations where each land surface model is emulated separately (Figure S1).

For peatland ΔC, three out of the five emulated models show positive correlation with increasing Tpeak (R^2 from 0.78 to 0.86), one does not show significant correlation with Tpeak (R^2 = 0.28), and one shows a negative correlation with Tpeak (R^2 = 0.93). For CO_2 fluxes from northern peatlands, three out of the five emulated models show a slight negative correlation with Tpeak (R^2 from 0.80 to 0.89), one does not show significant correlation with Tpeak (R^2 = 0.20), and one shows a positive correlation with Tpeak (R^2 = 0.93). Cumulative CH_4 emissions consistently exhibit a strong correlation with Tpeak (R^2 > 0.9) across all complex land surface models (Figure S1).

Climate feedback and budget reduction

In all evaluated scenarios, the warming of northern peatlands amplifies peak global temperature, resulting in an additional 0.02°C (0.01–0.02°C) for every 1°C of Tpeak increase (Figure 4A). This positive feedback from peatlands contributes to a reduction in the remaining carbon budget of 36.7 $GtCO_2$ (22.3–47.5 $GtCO_2$) per °C of Tpeak increase (Figure 4B).

Furthermore, this net positive climate feedback from northern peatlands also significantly prolongs the overshoot duration. Once peatland feedbacks are included in OSCAR, the GSAT stays above the targeted 1.5°C for 5 (4–8) more years in overshooting scenarios (Figure 4C). Temperature overshoot starts 1 year (0–1 year) earlier and ends years 5 years (4–8 years) later. The impact of peatland feedbacks on the overshoot duration increases with the global warming stabilization level: for scenarios overshooting 2.5°C, the inclusion of northern peatlands increases the overshoot duration by 13 years (9–27 years), with the it starting 3 years (1–4 years) earlier and ending 10 years (7–24 years) later (Table S2). The prolonged overshoot duration corresponds with an additional amount of carbon removal in order for the temperature anomaly to fall back below the target level. By including northern peatlands, the median requirement in carbon removal increases by 40 $GtCO_2$ (16–60 $GtCO_2$) if temperature overshoots 1.5°C. This corresponds with an 8.6% (5.2%–68%) relative increase in this removal requirement. Furthermore, this value increases by 60 $GtCO_2$ (32–95 $GtCO_2$) (or a 4.3% [1.8%–7.4%] relative increase) if temperature overshoots 2°C, and by 105 $GtCO_2$ (45–166 $GtCO_2$) (or a 4.2%

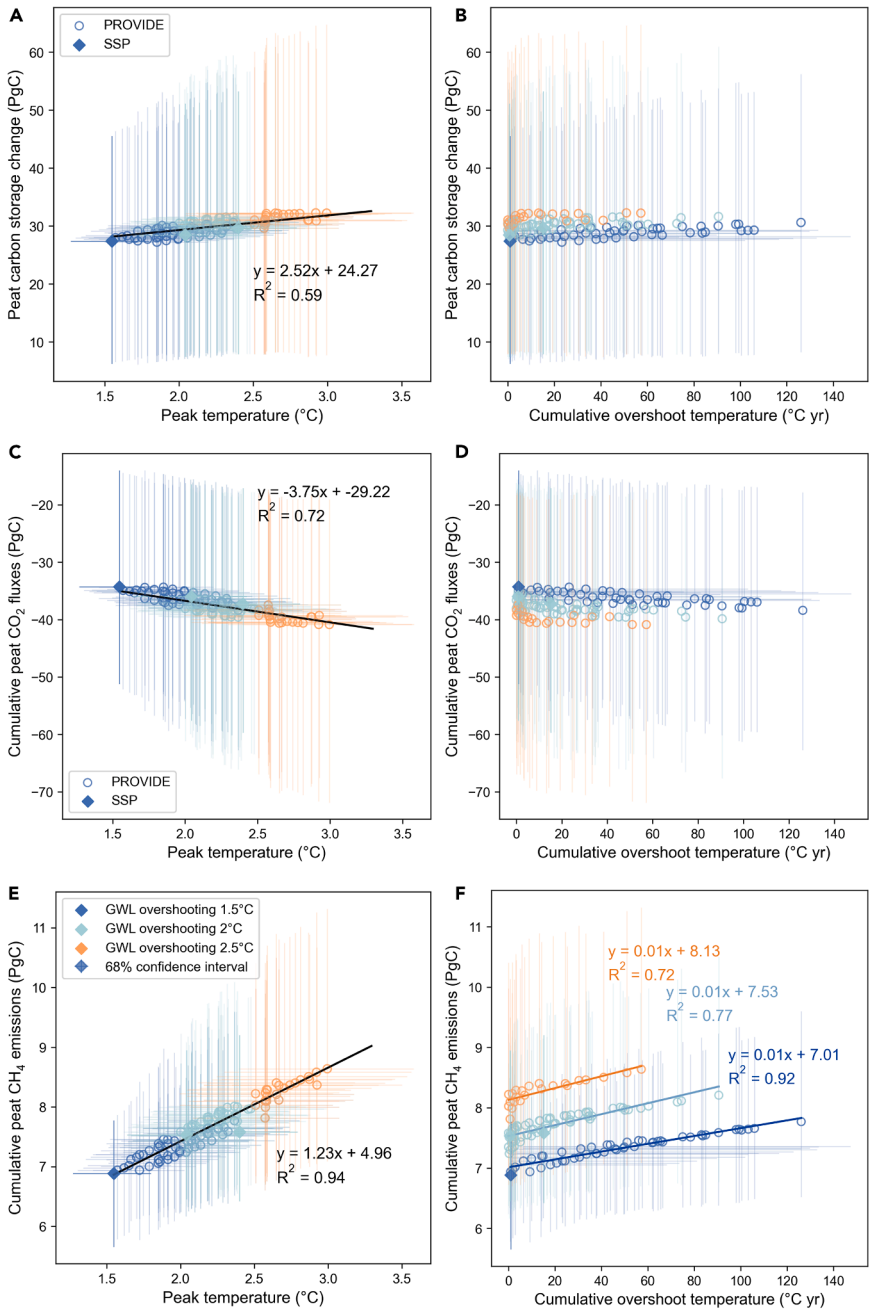

Figure 3. Cumulative changes in peatland carbon storage and emissions

The cumulation period is 2000–2300. We used 2 sets of scenarios: 8 SSPs and a set of 282 emission pathways called PROVIDE scenarios, with a focus on overshoot (202 of which exceed 1.5°C, 2°C. and 2.5°C global warming level before returning below).

(A) Cumulative carbon storage change in northern peatlands from 2000 to 2300 as a function of peak temperature.

(B) Cumulative carbon storage change in northern peatlands from 2000 to 2300 as a function of cumulative overshoot temperature.

(C) Cumulative peatland carbon dioxide (CO_2) flux (negative sign indicates a flux into peatland) as a function of peak temperature.

(D) Cumulative peatland CO_2 flux as a function of cumulative overshoot temperature.

(E) Cumulative peatland methane (CH_4) emissions as a function of peak temperature.

(F) Cumulative peatland CH_4 emissions as a function of cumulative overshoot temperature.

The colors correspond with global warming levels (GWLs) overshooting 1.5°C, 2°C, or 2.5°C. The uncertainty bars show the 68% CI of the full Monte Carlo simulation, which includes uncertainties from different peatland representations and from all other earth system processes included in OSCAR. The symbols show the best-guess estimates. Linear correlation parameters are given only when significant. Only overshoot scenarios are shown in this figure. The model differences are shown in Figure S1.

[1.6%–6.8%] relative increase) if the temperature overshoots 2.5°C (Figure 4D).

DISCUSSION

We incorporated northern peatlands into the reduced-complexity ESM OSCAR v3.1.2 and examined the feedback and its implications for the remaining carbon budget and carbon removal requirements. We explored a large range of scenarios that meet the goal of limiting temperature change below 1.5°C to 2.5°C by the 2300, with different characteristics and notably various temperature overshoots.

Overall, existing peatlands behave as a CO_2 sink and a CH_4 source in all explored scenarios. CH_4 emissions from peatlands increase with increasing temperature. The peatland CO_2 sink strength, particularly the turning point where the peatland CO_2 sink switches from increasing to decreasing, is governed by both temperature and atmospheric CO_2 concentration. This is also seen in the complex process-based peatland models, with four out of the five models predicting a similar behavior under the RCP8.5 scenario.[3] Nevertheless, the timing of this reversal varies significantly among the complex models (the LPJ-GUESS model projected that a switch had already happened around 2000, while LPJ-GUESS_dynP projected that the switch would take place in 2085), due to substantial differences in their representation of peatland carbon uptake by plants, and peat carbon decomposition in response to increased atmospheric CO_2 and warming.[3,22]

Our results reveal that although northern peatlands are projected to continue accumulating C, they exert positive feedback on the temperature overshoot that increases both peak temperature and overshoot duration. Earlier work by Qiu et al. (2022)[3] estimated that northern peatlands will remain a CO_2 sink and

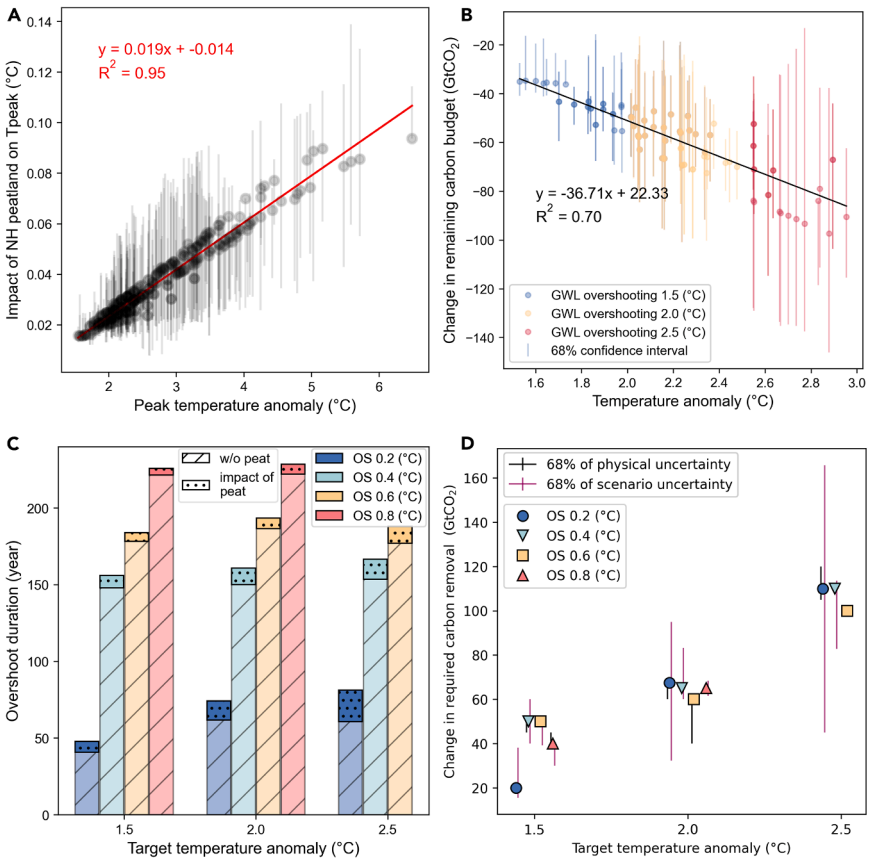

Figure 4. Northern peatlands' impact on peak temperature (Tpeak), carbon budget overshoot duration and required carbon removal

(A) The relationship between the impact of northern peatland greenhouse gas (GHG) fluxes on Tpeak. The uncertainty bars show the 68% CI of the full Monte Carlo simulation, which includes uncertainties from different peatland representations and from all other earth system processes included in OSCAR. The symbols show the best-guess estimates.

(B) The impact of northern peatlands on the remaining carbon budget. The colors correspond to global warming levels (GWLs) overshooting 1.5°C, 2°C, or 2.5°C. The symbols show the best-guess estimate.

(C) The (median) overshoot duration extension as a result of including northern peatlands. The colors represent the degree of overshoot ('OS' in figure), indicating the extent by which the peak temperature exceeds the target temperature anomaly;.

(D) The impact of northern peatlands on the required carbon removal. The symbols show the best-guess estimate.

maintain climate neutrality under a strong mitigation scenario RCP2.6. Under SSP1-2.6, a CMIP6 scenario comparable with RCP2.6, we project that northern peatlands will have a very small positive effect on global warming (exacerbating the peak temperature by 0.02°C [0.01–0.03°C]). In agreement with Qiu et al. (2022),[3] we project a substantial increase of CH_4 emissions from northern peatlands under high temperatures, which contribute to the positive feedback of peatlands on global warming. It should be noted that the climate feedback of peatlands in Qiu et al. (2022)[3] was estimated using offline simulations in which climate change itself was prescribed. In our study, this was estimated in a fully coupled (online) mode. Müller and Joos (2021)[4] predicted a slight decline of total peat carbon in scenario SSP1-2.6 and in SSP2-4.5, suggesting long-term net losses of peatland area and carbon. As peatland area change is not considered in our study, it is possible that carbon loss caused by peat area loss is overlooked. Thus, accounting for peatland area change could improve the peat carbon module. Furthermore, this new module and the existing wetland module of OSCAR (where peatlands and mineral-soil wetlands are not explicitly distinguished) were calibrated with different process-based models and under different simulations. We have tried to account for the overlapping issue by separating peatland and mineral-soil wetland areas, however, it is still possible that there is a double counting problem in the end result. A key area for future improvement is obtaining joint estimates of peatlands and mineral-soil wetlands responses from the same process-based models.

Our results provide a statistical best-guess estimate of future peatland response, although substantial uncertainty remains in the parameters calibrated from different process-based land surface models. This reveals the need to improve our understanding of peatland systems. The five structurally different land surface models used in our study were evaluated and tuned against historical and contemporary climate conditions. However, some of the scenario conditions (especially the high-overshoot scenarios) are well beyond the calibration conditions. A critical limitation of current process-based land surface models is their inability to fully capture the complex self-regulating nature of peatland systems. Specifically, peat accumulation or loss alters the height of the peat surface, which in turn affects the production-decomposition relationship. However, these land surface models do not adequately represent this dynamic feedback, leading to potential inaccuracies when peatlands are pushed beyond their stable operating ranges. The extent to which these land surface models (and therefore our own emulator) can robustly represent the response to such climate conditions remains uncertain. Moreover, there are uncertainties remaining in other parts of the Earth system processes. Since we evaluate the climate feedback of northern peatland with a fully coupled model, which has never been done before, the uncertainties from non-peatland processes are also incorporated in our results.

The five complex process-based models have shown considerable across-model spread in predicting the peatland carbon cycle (Figure S1). This variability is not unique to peatland models, and it has been ubiquitously observed across various model intercomparison efforts. For example, a large spread has been noted in the modeling of permafrost carbon dynamic.[23] This widespread variability highlights the importance of not only

developing increasingly complex models but also identifying and reducing the sources of model uncertainty and across-model spread. It is important to note that the inclusion of all five complex process-based models in the emulator was not intended for inter-model comparison; rather, the strength of the emulator lies in its ability to capture the full range of responses across these complex models.

To advance our understanding of peatland systems and to reduce modeling uncertainties, additional calibration of process-based models on observations are essential. For example, while some experiments have shown strong vulnerability of *Sphagnum* to northern peatland warming,[24] understanding of non-vascular plant feedbacks and the associated characterization of methanotroph response under warming of northern peatlands requires more extensive measurements and further model development. Additionally, all five complex process-based peatland models considered in this study focus solely on peatland carbon exchanges with the atmosphere; fluvial carbon fluxes (in the form of dissolved organic carbon [DOC] and particulate organic carbon) have not been taken into account. Observation-based studies have shown that DOC is the dominant form of peatland fluvial carbon, and global peatlands are estimated to contribute at least 91 ± 54 Tg DOC to surface water annually.[25] Furthermore, the important impact of wildfires on peatlands is not accounted for by any of the process-based models, thus not emulated by the peatland carbon emulator. The frequency and severity of wildfires are expected to increase with global warming. It is, therefore, important to explicitly model these processes in complex models to capture the whole peatland feedback.

We showed that, despite the ongoing accumulation of carbon and sustained CO_2 sequestration, peatlands could still constitute a positive (i.e., warming) feedback in the climate system. This emphasizes the importance of incorporating other potent greenhouse gasses in addition to CO_2 in evaluating ecosystem feedbacks. Furthermore, the specific focus on temperature overshoot in our study reveals the importance of accounting for the feedback from northern peatlands in both the remaining carbon budget and the carbon capture requirements. Various studies have highlighted the risks of temporary overshoots, including increasing risks of crossing the stability threshold of tipping elements of the Earth system[26,27] and of intensified sea level rise.[28] While the feedback from peatlands may seem modest in its contribution to peak temperature rise, its importance lies in presenting a substantial risk for extending the duration of overshoot, owing to its nonlinear behavior.

METHODS

As a reduced-complexity ESM, OSCAR was calibrated to emulate the behavior of complex ESMs at yearly timescale (without generating inter-annual variability). OSCAR uses anthropogenic emissions as inputs. The main model features the following key components: ocean carbon module, land carbon and other land processes module, climate-response module and atmospheric chemistry module. OSCAR v3.1.2 is still calibrated on CMIP5 ESMs.

We used OSCAR v3.1.2, which is a minor update of v3.1.[29] The full description of OSCAR v2.2, including its structure, equations and calibration can be found in Gasser et al. (2017).[30] The changes from v2.2 to v3.1 are detailed in Gasser et al. (2020).[29] In the historical period (1750–2014), OSCAR was driven by (1) global fossil emissions and other non-land-use-change greenhouse gas emissions from the CEDS-CMIP6 inventory,[31]; (2) N_2O emissions from PRIMAP (1850–1990) and the SSP-CMIP6 database[19–21] (1990–2014), and linearly extrapolated to zero to year 1750, (3) combined CH_4 emissions from CEDS-CMIP6[32] (1990–2014), SSP-CMIP6 database[19–21] (1990–2014) and PRIMAP[33] (1850–1970), linearly extrapolated to zero to 1750, (4) air pollutants' emissions (NOx, SO_2, VOC, BC, CO, NH_3, and OC) were scaled with the SSP-CMIP6 database[19–21] based on 2014, (5) halogenated compounds emissions from EDGARv6,[34] (6) additional radiative forcings (RFs) based on CMIP6,[35] and (7) land use change CO_2 emissions based on GCB 2021[36] (1750–2014). The OSCAR model was run in an emission-driven mode with the land-use change module turned off as emissions from land use change are prescribed with the aforementioned dataset.

In this study, OSCAR was run in a probabilistic fashion. Every single experiment was run for 2,000 different configurations of OSCAR, drawn randomly from the pool of all possible parameter values (excluding the peatland parameters) in a Monte Carlo setup.[34] Each set of the five peatland emulator parameters was combined with these 2,000 configurations, in addition to one set of simulations with the peatland module turned off. In total, 12,000 different configurations were run per experiment. This setup allows us to study the full uncertainty of the Earth system, with the possibility to separate the peatland parameters' contribution to the total uncertainty.

SSP and PROVIDE scenarios

The OSCAR model was run in emission-driven mode for the time period between 2015 and 2300. A total of 290 experiments were performed. We used two sets of scenarios: 8 SSPs and a set of 282 emission pathways crafted for the PROVIDE project (hereafter called PROVIDE scenarios).[18] Taken from the SSP scenario database,[20] the former are the default CMIP6 scenarios. The latter set was created specifically with a focus on overshoot (202 are overshoot scenarios for global warming levels of 1.5°C, 2°C, and 2.5°C).

The SSP extensions beyond 2100 are slightly modified from O'Neill et al. (2016).[37] For fossil CO_2 emissions, we extended the negative emissions beyond 2100 as described in Meinshausen et al. (2020),[38] with a ramp-up to zero emissions at the latest by 2250. We updated land use change CO_2 emissions based on Meinshausen et al. (2020)[38] to linearly extend emissions to zero from the 2100 to 2150 and to remain zero until 2300. Additional RFs follow Quilcaille et al. (2023).[35]

The set of PROVIDE scenarios was specifically created to evaluate various overshoot pathways. The method to generate the scenarios was described in Lamboll et al. (2022).[18] The scenarios follow different mitigation pathways for fossil CO_2 and CH_4 emissions. For other emissions, the emission pathways were set by default to the SSP1-1.9 level. In general, the fossil CO_2 emission levels were designed to follow one of the baseline emission pathways (SSP2-4.5, SSP3-6.0, and SSP5-baseline) until the year when mitigation starts (2030, 2040, and 2050). The emissions then linearly declined until the year when zero CO_2 emissions are reached (2040, 2060, 2080, 2100, 2150,

and 2200). As a next step, fossil CO_2 emissions either stayed at zero or were linearly reduced to one of the negative emission levels (-5 PgC y^{-1} and -10 PgC y^{-1}) following a gradient no faster than the fastest in the SR1.5 database.[39,40] Thereafter, the fossil CO_2 emission levels remained unchanged until 2300. The CH_4 emission mitigation level was associated with the fossil CO_2 emissions with variations (low and high).

Northern peatland carbon emulator

We coupled a peatland carbon emulator to OSCAR v3.1.2, calibrated on five state-of-the-art peatland models: LPJ-MPI, ORCHIDEE-PEAT, LPX-Bern, LPJ-GUESS, and LPJ-GUESS_dynP (dynP for dynamic multi-peat layers). As described in Qiu et al. (2022),[3] these complex peatland models show substantial differences in their representation of peatland vegetation, peat carbon pools and carbon fluxes, as well as peatland soil thermal and hydraulic processes. For example, four out of these five models (except ORCHIDEE-PEAT) have detailed representation of northern peatland vegetation, including Sphagnum, flood-tolerant grasses, shrubs, and trees. The parameterization of peatland vegetation in ORCHIDEE-PEAT uses only one grass-like plant functional type to represent the average of vegetation growing in intact northern peatlands. The models included in this analysis include runoff and drainage essential for simulating the water balance of ombrogenic peatlands that are known to be especially important for regional CO_2 and CH_4 fluxes. The hydrological, thermal, and carbon-related features of these models are summarized in Figure S3 and in Tables S1–S3 of Qiu et al. (2022).[3] A concise summary of model details is provided in Note S1. The northern peatland carbon emulator takes these different representations of northern peatland into account implicitly through different parameter values calibrated on the different process-based models.

The calibration of the parameters defined hereafter was done using outputs of the complex models for integrations over 1850–2300 of the RCP8.5, RCP2.6, control (in which atmospheric CO_2, and climate conditions are maintained at their pre-industrial level) and RCP8.5-bgc (in which climate conditions are maintained at their pre-industrial level but atmospheric CO_2 increases with time according to the RCP8.5 scenario).[3] Northern peatlands (peatlands north of 30°N latitude) from PEATMAP[41] were aggregated into four sub-regions: permafrost North American peatlands, non-permafrost North American peatlands, permafrost Eurasian peatlands, and non-permafrost Eurasian peatlands. Among the five complex models, LPJ-MPI does not explicitly consider permafrost processes. Therefore, there are only two regions defined for LPJ-MPI. All five complex models and four peatland sub-regions are emulated by the same set of governing equations described below (Equations 1–9), but with different parameter values (Table S3). The peat carbon emulator is fully defined by these equations and parameter values.

First, we modeled the regional air surface temperature change (ΔT^i) in each sub-region i with a linear dependency on global temperature change (ΔT):

$$\Delta T^i = \omega^i \Delta T. \quad \text{(Equation 1)}$$

The parameters ω^i were calibrated with a linear fit between ΔT^i and ΔT (Figure S2). The temperature change is defined as temperature difference as compared to the pre-industrial level, which is taken as the average over 1861–1900. It represents a feature of the climate system, rather than the feature of the land surface models.

Second, we calibrated the northern peatland net primary production (NPP) via a fertilization function (F_{fert}) and changes in local surface temperature (ΔT^i) with assumed linear sensitivities, which is split between a first-order term ($\gamma_{npp,T1}$) and a second-order term ($\gamma_{npp,T2}$) (Figure S3).

$$\Delta npp^i = npp_0^i \left(\frac{F_{fert}^i[\Delta C]}{1+\gamma_{npp,T1}^i * \Delta T^i - \gamma_{npp,T2}^i * \Delta T^{i2}} - 1 \right), \quad \text{(Equation 2)}$$

where npp_0 is the pre-industrial NPP taken as the average over 1861–1900. The functional form of F_{fert} is a combination of logarithmic and linear sensitivities:

$$F_{fert}^i = \frac{1+\beta_{npp1}^i \, ln\left(\frac{\Delta C}{C_0}+1\right)}{1+\beta_{npp2}^i \frac{\Delta C}{C_0}}, \quad \text{(Equation 3)}$$

where β_{npp1} and β_{npp2} are, respectively, fertilization and down-regulation terms to global atmospheric CO_2 concentration change (ΔC) relative to pre-industrial level (C_0).

Third, we calibrated the heterotrophic respiration rate (rho^i) as a function with linear dependency on the mortality flux change (Δf_{mort}) (Figure S4). The dependency on the ΔT^i follows a Gaussian function, as has been previously discussed by Tuomi et al. (2008)[42] and Gasser et al. (2018)[43]:

$$rho^i = rho_0^i \left(1 + \gamma_{mort}^i \frac{\Delta f_{mort}^i}{\Delta f_{mort,0}^i}\right) exp\left(\gamma_{T1}^i \Delta T^i + \gamma_{T2}^i \Delta T^{i2}\right). \quad \text{(Equation 4)}$$

rho_0 is the pre-industrial heterotrophic respiration rate taken as the average over 1851–1900. γ_{mort}, γ_{T1}, and γ_{T2} are the sensitivity parameters. The first-order term in the Gaussian function is an approximation of the Q10 dependence. The second order term in the Gaussian function represents saturation, an important property for the peatland systems under high warming scenarios (as illustrated by the curve flattening in Figure S4).

Fourth, we calibrated the mortality rate (μ) to vegetation carbon (Figure S5). It is calibrated assuming linear dependency on npp or C_{veg}, and linear dependency on ΔT^i with a first-order and a second-order term:

$$\mu^i = \mu_0^i \left(1 + \alpha_{npp}^i * \frac{npp^i}{npp_0^i} + \alpha_{C_{veg}}^i * \frac{C_{veg}^i}{C_{veg,0}^i}\right) * \left(1 + \varepsilon_{T1}^i \Delta T^i + \varepsilon_{T2}^i \Delta T^{i2}\right). \quad \text{(Equation 5)}$$

μ_0 and $C_{veg,0}$ are the pre-industrial mortality rate and vegetation carbon pool taken as the average over 1851–1900, respectively. α_{npp}, $\alpha_{C_{veg}}$, ε_{T1}, and ε_{T2} are sensitivity parameters. Following *ad hoc* testing, $\alpha_{C_{veg}}$ is forced to zero for LPX-Bern

and ORCHIDEE, and α_{npp} is forced to zero for LPJ-MPI, LPJ-GUESS and LPJ-GUESS_dynP.

Fifth, we calibrated the CH_4 flux (f_{met}) as a function assuming logarithmic dependency on heterotrophic respiration (rh) (Figure S6). The dependency on the ΔT^i follows a Gaussian function:

$$f^i_{met} = f^i_{met,0}\left(1 + \gamma^j_{rh}\, ln\left(\frac{rh^i}{rh^i_0}\right)\right) * \exp\left(\eta^j_{T1}\Delta T^i + \eta^j_{T2}\Delta T^{i2}\right). \quad \text{(Equation 6)}$$

$f_{met,0}$ and rh_0 are the pre-industrial CH_4 flux and heterotrophic respiration taken as the average over 1851–1900, respectively. γ_{rh}, η_{T1}, and η_{T2} are sensitivity parameters.

Sixth, we computed the two carbon pools: the vegetation carbon pool (C_{veg}) and the soil carbon pool (C_{soil}) . C_{veg} changes with time following NPP and f_{mort} change:

$$\frac{dC^i_{veg}}{dt} = \left(npp^i - npp^i_0\right) - \left(f^i_{mort} - f^i_{mort,0}\right). \quad \text{(Equation 7)}$$

The change in C_{soil} with time follows the change in f_{mort} and rh:

$$\frac{dC^i_{soil}}{dt} = \left(f^i_{mort} - f^i_{mort,0}\right) - \left(rh^i - rh^i_0\right). \quad \text{(Equation 8)}$$

Finally, the peatland CO_2 flux (f_{CO2}) was deduced as:

$$f^i_{CO2} = f^i_{CO2,0} - \left(npp^i - npp^i_0\right) + \left(rh^i - rh^i_0\right) - \left(f^i_{met} - f^i_{met,0}\right). \quad \text{(Equation 9)}$$

The $f^i_{CO2,0}$ is the pre-industrial CO_2 flux taken as the average over 1851–1900.

The overall performance of the emulator is shown in Figure S7, with the emulator driven by the emulated model's global atmospheric CO_2 concentration change and global temperature change. The performance has been assessed as satisfactory, with deviations represented by normalized root-mean-square errors of less than 15% (Figure S7).

To evaluate whether the peatland emulator can capture the behavior of complex peatland models under overshoot scenarios, bias-corrected climate projections by the IPSL-CM6A-LR ESM for the SSP5-3.4 overshoot scenario (from ISIMIP3b[44]) were used to drive OSCAR and ORCHIDEE-PEAT. This scenario was not used to calibrate the emulator.

While systematic deviations (from historical observations) in the ESM data have been carefully corrected in this climate forcing (hereafter called ISIMIP3b corrected), it ends in 2100 and is too short to reveal the full peatland responses to warming given the slow turnover of peatland carbon pools.[4] Therefore, the projected climate by the IPSL-CM6A-LR ESM for the same SSP5-3.4 overshoot scenario but extended to the year 2300 were bias corrected following Zhang et al. (2019)[45] (hereafter called Zhang et al. corrected) and used to drive OSCAR and ORCHIDEE-PEAT. As shown in Figure S8, under the SSP5-3.4 overshoot scenario and with both climate forcings (ISIMIP3b corrected and Zhang et al. corrected), projected changes in peatland C fluxes by the complex model ORCHIDEE-PEAT are reasonably well reproduced by the peatland emulator in OSCAR.

Constraining Monte Carlo ensemble and uncertainty calculation

Each configuration of OSCAR is a combination of equations and parameters that are drawn randomly from a pool of potential parameterizations. While this Monte Carlo setup takes account of uncertainties in different parameterizations of ESMs, it can result in a combination of physically inconsistent modules in a given configuration. Therefore, it can cause a large spread between configurations and a difference between the average of configurations and the average of outputs of complex models that are used for calibration.[29,30,35]

To constrain the spread and bias in raw outputs of OSCAR configurations, we gave each configuration a weight according to how well it compares to historical observations (Equation 10, Gasser et al. [2020][29] and their Appendix A5).

$$\omega(x) = \frac{1}{\sigma\sqrt{2\pi}} exp\left(-\frac{(x-\mu)^2}{2\sigma^2}\right), \quad \text{(Equation 10)}$$

where μ and σ are the mean and SD of the observation, and x is the simulated value.

Three observationally based datasets[5] were used as constraints: GSAT change from the period of 1850–1900 to the period of 1995–2014 is used to constrain the climate system; the atmospheric CO_2 concentration change from pre-industrial to the period of 2010–2019 and the atmospheric CH_4 concentration change from pre-industrial to the period of 2008–2017 are used to constrain the carbon cycle. We calculated a weight factor for each of these three constraints, that is $\omega(x_{GSAT})$, $\omega(x_{CO2})$ and $\omega(x_{CH4})$, and the final constraining weight is the multiplication of these three weight factors.

For the calculation of $\omega(x_{GSAT})$, the observed μ is 0.85°C and the observed σ is 0.09°C (IPCC AR6, Cross Chapter Box 2.3).[5] We added 0.1°C to the observed σ given that OSCAR does not endogenously simulate inter-annual variability of GSAT. For the calculation of $\omega(x_{CO2})$ and $\omega(x_{CH4})$, the observed μ is 131.7 ppm and 1107.3 ppb, respectively (IPCC AR6, Figure 5.12 and Figure 5.14).[5] However, in the emission-driven mode, OSCAR uses a single emission trajectory for the historical period (see the OSCAR v3.1.2 section), thereby neglecting uncertainties in anthropogenic CO_2 and CH_4 emissions. Therefore, for the calculation of $\omega(x_{CO2})$ and $\omega(x_{CH4})$, σ of anthropogenic sources are used instead of the (very low) σ of observations. According to IPCC AR6 (Table 5.2),[5] the uncertainty range of anthropogenic CH_4 emissions for the 2008–2017 period is 48 $TgCH_4\ y^{-1}$ (minimum-maximum values from bottom-up estimates). Assuming that this minimum-maximum range approximately equal to 95% CI and the atmospheric lifetime of CH_4 is 9.1 years (IPCC AR6, Table 6.2),[5] the calculated σ anthropogenic CH_4 is 77.3 ppb. For the long-lived climate forcer CO_2, we consider cumulative airborne fraction from pre-industrial to the period of 2010–2019. According to IPCC AR6 (Table 5.1),[5] the cumulative CO_2 emissions is 685 ± 75 PgC, with 285 ± 5 PgC remaining in the atmosphere; thus, the airborne fraction of CO_2 is 0.42. Applying this airborne fraction of CO_2 to the uncertainty of the cumulative CO_2 emissions (75 PgC), the calculated σ of anthropogenic CO_2 is 13.7 ppm.

As shown in Figure S9, raw outputs of OSCAR are well constrained by observations. The simulated GSAT change from

1850–1900 to 1995–2014 is constrained to 0.91 ± 0.15°C, close to the constraint (0.85 ± 0.19°C). Without the constraint, the simulated value is 1.08 ± 0.38°C. The simulated atmospheric CO_2 change from pre-industrial to 2010–2019 is constrained to 128.7 ± 12.7 ppm (constraint, 131.7 ± 13.7 ppm), and the simulated atmospheric CH_4 change from pre-industrial to 2008–2017 is constrained to 1,138.1 ± 68.1 ppb (constraint, 1,107.3 ± 77.3 ppb). Without the constraint, the simulated atmospheric CO_2 and CH_4 changes are 135.1 ± 21.8 ppm and 1,381.7 ± 238.1 ppb, respectively.

As described by Quilcaille et al. (2023),[35] the ocean carbon cycle module is unstable under high-CO_2 and high-warming scenarios, causing a numerical divergence and a physically unrealistic oscillation of the oceanic carbon sink in some configurations. Following Quilcaille et al. (2023),[35] we identified and excluded 129 (out of 2,000) configurations for which the ocean sink of SSP3-7.0 diverged and oscillated (illustrations of simulated ocean carbon sink; see Figure S10). Then, we used the remaining 1,871 configurations as a common set of configurations for all experiments (Figure S9). In simulations using the OSCAR-peat modules, equal weights are assigned to the contributions of parameters calibrated from each ESM. All results in this study are presented as the weighted averages (noted as the best-guess values in results), weighted standard deviations and weighted CI of these 1,871 configurations and 5 peatland models unless specified otherwise.

Remaining carbon budgets and carbon removal requirement calculation

The remaining allowable carbon emissions for a given global warming level is calculated based on the near-linear relationship between cumulative CO_2 emissions and warming. For overshoot scenarios, cumulative emissions of CO_2 reach the maximum at the peak temperature. To bring the temperature back down below a given climate target, the amount of carbon to be captured (B_c) is:

$$B_c = \left(T_{peak} - T_{target}\right) \times TCRE, \quad \text{(Equation 11)}$$

where $TCRE$ is the amount of warming per unit of cumulative CO_2 emissions (1.65°C per 1,000 PgC, IPCC AR6), T_{peak} is the peak temperature anomaly (compared with present warming) in the overshoot scenario and T_{target} is the targeted temperature.

In this study, the absolute impact of peatlands on the remaining carbon budget is quantified as the difference between the experiments with the peatland module turned on and turned off:

$$\Delta B = B_{c,with\ peat} - B_{c,without\ peat} \quad \text{(Equation 12)}$$

where $B_{c,with\ peat}$ and $B_{c,without\ peat}$ is the net overshoot C budget when the peatland module is turned on and turned off, respectively.

The required carbon removal (R_c) is calculated for each scenario, as the amount of CO_2 removal needed when the temperature target is overshot. Specifically, it is calculated as the cumulative anthropogenic negative emissions from the year of net zero until the end of the overshoot duration. The absolute impact of peatlands on the net carbon removal requirement is quantified as the difference between the experiments with the peatland module turned on and turned off:

$$\Delta R_c = R_{c,with\ peat} - R_{c,without\ peat} \quad \text{(Equation 13)}$$

RESOURCE AVAILABILITY

Lead contact

Requests for further information and resources should be directed to and will be fulfilled by the lead contact, Biqing Zhu (zhub@iiasa.ac.at).

Materials availability

This study did not generate new unique materials.

Data and code availability

The code and processed data used to generate all the results of this study are available at https://github.com/bq-zhu/ms-peat-overshoot. The source code of OSCAR is available at https://github.com/tgasser/OSCAR. The source code of the peatland emulator is available from the corresponding author upon request.

ACKNOWLEDGMENTS

C.Q. acknowledges the financial support from the National Key R&D Program of China (2022YFF0802104). B.Z. and T.G. acknowledge support from the European Union's Horizon 2020 research and innovation program under grant agreement #773421 (Nunataryuk project) and support from European Union's Horizon Europe research and innovation program under grant agreement #101056939 (RESCUE project). B.Z., T.G. and P.C. acknowledge support from the European Union's Horizon 2020 research and innovation program under grant agreement #101003687 (PROVIDE project). T.G. was also supported through the Woodwell Climate Research Center by the Quadrature Climate Foundation (QCF Prime Grant Number 01-21-000094). P.C. is supported by the CALIPSO project funded by the generosity of Schmidt Sciences. K.T. benefited from state assistance managed by the National Research Agency in France under the Programme d'Investissements d'Avenir under the reference ANR-19-MPGA-0008. J.C. was supported by the National Key Research and Development Program of China (2022YFF0801904). T.K. acknowledges support from the "PalMod" project, funded by the German Federal Ministry of Education and Research (BMBF) (01LP1921A), and from the European Research Council (ERC) under the European Union's Horizon 2020 research and innovation program (grant agreement No 951288, Q-Arctic). D.W. acknowledges support from the strategic research areas Modeling the Regional and Global Earth System (MERGE) at Lund University. D.W. received financial support from the H2020 CRESCENDO project (grant agreement no. 641816). LPJ-GUESS simulations were enabled by resources provided by the Swedish National Infrastructure for Computing (SNIC) at LUNARC partially funded by the Swedish Research Council through grant agreement no. 2018-05973. B.G. was supported by the grant "Holistic management practices, modeling and monitoring for European forest soils" (H2020 grant agreement 101000289). N.J.S. acknowledges the funding from the Ministry of Agriculture and Forestry Finland (Project NC-GRASS: VN/28562/2020-MMM-2). N.C. acknowledges funding by the Nunataryuk (EU grant agreement no. 773421) and the Swedish Research Council FORMAS (contract no. 2019-01151). LPJ-GUESS_dyn simulations were performed on the supercomputing facilities at the University of Oslo, Norway, and on the Aurora and Tetralith resources of the Swedish National Infrastructure for Computing (SNIC) at the Lund University Center for Scientific and Technical Computing (Lunarc), project no. 2021/2-61, 2022/6-65 and no. 2021/2-28, and Linköping University, project no. snic2020/5-563. N.C. acknowledges support from the strategic research areas Modeling the Regional and Global Earth System (MERGE) and Biodiversity and Ecosystem Services in a Changing Climate (BECC) at Lund University. N.C. acknowledges support from the Swedish Research Council FORMAS grant (contract no. 2019-01151), BECC, MERGE. A.B. and M.J.K. were supported by the French MOPGA Process Oriented Model Evaluation with Land Observations (POMELO). W.Z. was supported by the grants from the Swedish Research Council VR 2020–05338

and Swedish National Space Agency 209/19. A.G.S. acknowledges funding from the European Research Council (ERC) under the European Union's Horizon 2020 research and innovation program (grant agreement No 865403). G.S. acknowledges support from the Novo Nordisk Foundation, grant NNF23OC0081089. F.J. acknowledges funding from the Swiss National Science Foundation (project no. 200020_200511). Y.Z. received support from the Joint Chinese Academy of Sciences (CAS)-Max Planck Society (MPG) Research Project (grant no. HZXM20225001MI-3). E.S. was supported by the GreenFeedBack project funded by the European Union's Horizon Europe research and innovation program under grant agreement #101056921. S.W. acknowledges the BioGov project, funded by the Research Council of Norway (project no. 323945).

AUTHOR CONTRIBUTIONS

T.G. and P.C. designed the research; C.Q. and B.Z. conducted data analysis, with help from T.G. and P.C.; B.Z. and C.Q. drafted the manuscript; C.Q. coordinated the land surface model simulations and performed ORCHIDEE-PEAT simulations; B.Z. developed the OSCAR-peat module, coordinated the scenario development, and performed simulations with OSCAR and OSCAR-peat; R.L. developed the PROVIDE scenarios. N.C., T.K., J.M., and W.Z. performed LPJ-GUESS_dynP, LPJ-MPI, LPX-Bern, and LPJ-GUESS simulations, respectively. J.C., Y.Z., and I.M. prepared climate forcings for ORCHIDEE-PEAT; A.G.S. provided the observational dataset for Qiu et al. (2022).[3] All authors contributed to the interpretation of the results, drafting of the manuscript, and its revision.

DECLARATION OF INTERESTS

The authors declare no competing interests.

SUPPLEMENTAL INFORMATION

Supplemental information can be found online at https://doi.org/10.1016/j.oneear.2025.101353.

Received: January 30, 2024
Revised: October 3, 2024
Accepted: June 5, 2025
Published: July 1, 2025

REFERENCES

1. Yu, Z.C. (2012). Northern peatland carbon stocks and dynamics: a review. Biogeosciences *9*, 4071–4085. https://doi.org/10.5194/bg-9-4071-2012.
2. Hugelius, G., Loisel, J., Chadburn, S., Jackson, R.B., Jones, M., MacDonald, G., Marushchak, M., Olefeldt, D., Packalen, M., Siewert, M. B., et al. (2020). Large stocks of peatland carbon and nitrogen are vulnerable to permafrost thaw. Proc. Natl. Acad. Sci. USA *117*, 20438–20446. https://doi.org/10.1073/pnas.1916387117.
3. Qiu, C., Ciais, P., Zhu, D., Guenet, B., Chang, J., Chaudhary, N., Kleinen, T., Li, X., Müller, J., Xi, Y., et al. (2022). A strong mitigation scenario maintains climate neutrality of northern peatlands. One Earth *5*, 86–97. https://doi.org/10.1016/j.oneear.2021.12.008.
4. Müller, J., and Joos, F. (2021). Committed and projected future changes in global peatlands – continued transient model simulations since the Last Glacial Maximum. Biogeosciences *18*, 3657–3687. https://doi.org/10.5194/bg-18-3657-2021.
5. Intergovernmental Panel On Climate Change (2023). Climate Change 2021 – the Physical Science Basis: Working Group I Contribution to the Sixth Assessment Report of the Intergovernmental Panel on Climate Change, 1st ed. (Cambridge University Press). https://doi.org/10.1017/9781009157896.
6. Kikstra, J.S., Nicholls, Z.R.J., Smith, C.J., Lewis, J., Lamboll, R.D., Byers, E., Sandstad, M., Meinshausen, M., Gidden, M.J., Rogelj, J., et al. (2022). The IPCC sixth assessment report WGIII climate assessment of mitigation pathways: From emissions to global temperatures. Geosci. Model Dev. *15*, 9075–9109. https://doi.org/10.5194/gmd-15-9075-2022.
7. Chaudhary, N., Zhang, W., Lamba, S., and Westermann, S. (2022). Modeling pan-arctic peatland carbon dynamics under alternative warming scenarios. Geophys. Res. Lett. *49*, e2021GL095276. https://doi.org/10.1029/2021GL095276.
8. Qiu, C., Zhu, D., Ciais, P., Guenet, B., Peng, S., Krinner, G., Tootchi, A., Ducharne, A., and Hastie, A. (2019). Modelling northern peatland area and carbon dynamics since the Holocene with the ORCHIDEE-PEAT land surface model (SVN r5488). Geosci. Model Dev. *12*, 2961–2982. https://doi.org/10.5194/gmd-12-2961-2019.
9. Qiu, C., Zhu, D., Ciais, P., Guenet, B., Krinner, G., Peng, S., Aurela, M., Bernhofer, C., Brümmer, C., Bret-Harte, S., et al. (2018). ORCHIDEE-PEAT (revision 4596), a model for northern peatland CO2, water, and energy fluxes on daily to annual scales. Geosci. Model Dev. *11*, 497–519. https://doi.org/10.5194/gmd-11-497-2018.
10. Stocker, B.D., Spahni, R., and Joos, F. (2014). DYPTOP: a cost-efficient TOPMODEL implementation to simulate sub-grid spatio-temporal dynamics of global wetlands and peatlands. Geosci. Model Dev. *7*, 3089–3110. https://doi.org/10.5194/gmd-7-3089-2014.
11. Spahni, R., Joos, F., Stocker, B.D., Steinacher, M., and Yu, Z.C. (2013). Transient simulations of the carbon and nitrogen dynamics in northern peatlands: from the Last Glacial Maximum to the 21st century. Clim. Past *9*, 1287–1308. https://doi.org/10.5194/cp-9-1287-2013.
12. Kleinen, T., Brovkin, V., and Schuldt, R.J. (2012). A dynamic model of wetland extent and peat accumulation: results for the Holocene. Biogeosciences *9*, 235–248. https://doi.org/10.5194/bg-9-235-2012.
13. Müller, J., and Joos, F. (2020). Global peatland area and carbon dynamics from the Last Glacial Maximum to the present – a process-based model investigation. Biogeosciences *17*, 5285–5308. https://doi.org/10.5194/bg-17-5285-2020.
14. McGuire, A.D., Christensen, T.R., Hayes, D., Heroult, A., Euskirchen, E., Kimball, J.S., Koven, C., Lafleur, P., Miller, P.A., Oechel, W., et al. (2012). An assessment of the carbon balance of Arctic tundra: comparisons among observations, process models, and atmospheric inversions. Biogeosciences *9*, 3185–3204. https://doi.org/10.5194/bg-9-3185-2012.
15. Smith, B., Wårlind, D., Arneth, A., Hickler, T., Leadley, P., Siltberg, J., and Zaehle, S. (2014). Implications of incorporating N cycling and N limitations on primary production in an individual-based dynamic vegetation model. Biogeosciences *11*, 2027–2054. https://doi.org/10.5194/bg-11-2027-2014.
16. Chaudhary, N., Miller, P.A., and Smith, B. (2017). Modelling past, present and future peatland carbon accumulation across the pan-Arctic region. Biogeosciences *14*, 4023–4044. https://doi.org/10.5194/bg-14-4023-2017.
17. Chaudhary, N., Miller, P.A., and Smith, B. (2017). Modelling Holocene peatland dynamics with an individual-based dynamic vegetation model. Biogeosciences *14*, 2571–2596. https://doi.org/10.5194/bg-14-2571-2017.
18. Lamboll, R., Rogelj, J., and Schleussner, C.-F. (2022). A guide to scenarios for the PROVIDE project (Climatology (Global Change)) https://doi.org/10.1002/essoar.10511875.2.
19. Rogelj, J., Popp, A., Calvin, K.V., Luderer, G., Emmerling, J., Gernaat, D., Fujimori, S., Strefler, J., Hasegawa, T., Marangoni, G., et al. (2018). Scenarios towards limiting global mean temperature increase below 1.5°C. Nat. Clim. Change *8*, 325–332. https://doi.org/10.1038/s41558-018-0091-3.
20. Riahi, K., van Vuuren, D.P., Kriegler, E., Edmonds, J., O'Neill, B.C., Fujimori, S., Bauer, N., Calvin, K., Dellink, R., Fricko, O., et al. (2017). The Shared Socioeconomic Pathways and their energy, land use, and greenhouse gas emissions implications: An overview. Glob. Environ. Change *42*, 153–168. https://doi.org/10.1016/j.gloenvcha.2016.05.009.
21. Gidden, M.J., Riahi, K., Smith, S.J., Fujimori, S., Luderer, G., Kriegler, E., Van Vuuren, D.P., Van Den Berg, M., Feng, L., Klein, D., et al. (2019). Global emissions pathways under different socioeconomic scenarios for use in CMIP6: a dataset of harmonized emissions trajectories through the end of the century. Geosci. Model Dev. *12*, 1443–1475. https://doi.org/10.5194/gmd-12-1443-2019.

22. Kwon, M.J., Ballantyne, A., Ciais, P., Qiu, C., Salmon, E., Raoult, N., Guenet, B., Göckede, M., Euskirchen, E.S., Nykänen, H., et al. (2022). Lowering water table reduces carbon sink strength and carbon stocks in northern peatlands. Glob. Change Biol. *28*, 6752–6770. https://doi.org/10.1111/gcb.16394.

23. McGuire, A.D., Genet, H., Lyu, Z., Pastick, N., Stackpoole, S., Birdsey, R., D'Amore, D., He, Y., Rupp, T.S., Striegl, R., et al. (2018). Assessing historical and projected carbon balance of Alaska: A synthesis of results and policy/management implications. Ecol. Appl. *28*, 1396–1412. https://doi.org/10.1002/eap.1768.

24. Petro, C., Carrell, A.A., Wilson, R.M., Duchesneau, K., Noble-Kuchera, S., Song, T., Iversen, C.M., Childs, J., Schwaner, G., Chanton, J.P., et al. (2023). Climate drivers alter nitrogen availability in surface peat and decouple N_2 fixation from CH_4 oxidation in the *Sphagnum* moss microbiome. Glob. Change Biol. *29*, 3159–3176. https://doi.org/10.1111/gcb.16651.

25. Rosset, T., Binet, S., Rigal, F., and Gandois, L. (2022). Peatland dissolved organic carbon export to surface waters: Global significance and effects of anthropogenic disturbance. Geophys. Res. Lett. *49*, e2021GL096616. https://doi.org/10.1029/2021GL096616.

26. Wunderling, N., Staal, A., Sakschewski, B., Hirota, M., Tuinenburg, O.A., Donges, J.F., Barbosa, H.M.J., and Winkelmann, R. (2022). Recurrent droughts increase risk of cascading tipping events by outpacing adaptive capacities in the Amazon rainforest. Proc. Natl. Acad. Sci. USA *119*, e2120777119. https://doi.org/10.1073/pnas.2120777119.

27. Wunderling, N., Winkelmann, R., Rockström, J., Loriani, S., Armstrong McKay, D.I., Ritchie, P.D.L., Sakschewski, B., and Donges, J.F. (2023). Global warming overshoots increase risks of climate tipping cascades in a network model. Nat. Clim. Change *13*, 75–82. https://doi.org/10.1038/s41558-022-01545-9.

28. Mengel, M., Nauels, A., Rogelj, J., and Schleussner, C.-F. (2018). Committed sea-level rise under the Paris Agreement and the legacy of delayed mitigation action. Nat. Commun. *9*, 601. https://doi.org/10.1038/s41467-018-02985-8.

29. Gasser, T., Crepin, L., Quilcaille, Y., Houghton, R.A., Ciais, P., and Obersteiner, M. (2020). Historical CO2 emissions from land use and land cover change and their uncertainty. Biogeosciences *17*, 4075–4101. https://doi.org/10.5194/bg-17-4075-2020.

30. Gasser, T., Peters, G.P., Fuglestvedt, J.S., Collins, W.J., Shindell, D.T., and Ciais, P. (2017). Accounting for the climate–carbon feedback in emission metrics. Earth Syst. Dyn. *8*, 235–253. https://doi.org/10.5194/esd-8-235-2017.

31. Feng, L., Smith, S.J., Braun, C., Crippa, M., Gidden, M.J., Hoesly, R., Klimont, Z., Van Marle, M., Van Den Berg, M., and Van Der Werf, G.R. (2020). The generation of gridded emissions data for CMIP6. Geosci. Model Dev. *13*, 461–482. https://doi.org/10.5194/gmd-13-461-2020.

32. Hoesly, R.M., Smith, S.J., Feng, L., Klimont, Z., Janssens-Maenhout, G., Pitkanen, T., Seibert, J.J., Vu, L., Andres, R.J., Bolt, R.M., et al. (2018). Historical (1750–2014) anthropogenic emissions of reactive gases and aerosols from the Community Emissions Data System (CEDS). Geosci. Model Dev. *11*, 369–408. https://doi.org/10.5194/gmd-11-369-2018.

33. Gütschow, J., Jeffery, M.L., Gieseke, R., Gebel, R., Stevens, D., Krapp, M., and Rocha, M. (2016). The PRIMAP-hist national historical emissions time series. Earth Syst. Sci. Data *8*, 571–603. https://doi.org/10.5194/essd-8-571-2016.

34. Monforti Ferrario, F., Crippa, M., Guizzardi, D., Muntean, M., Schaaf, E., Lo Vullo, E., Solazzo, E., Olivier, J., and Vignati, E. (2021). EDGAR v6.0 Greenhouse Gas Emissions (European Commission, Joint Research Centre (JRC)).

35. Quilcaille, Y., Gasser, T., Ciais, P., and Boucher, O. (2023). CMIP6 simulations with the compact Earth system model OSCAR v3.1. Geosci. Model Dev. *16*, 1129–1161. https://doi.org/10.5194/gmd-16-1129-2023.

36. Friedlingstein, P., Jones, M.W., O'Sullivan, M., Andrew, R.M., Bakker, D.C.E., Hauck, J., Le Quéré, C., Peters, G.P., Peters, W., Pongratz, J., et al. (2022). Global Carbon Budget 2021. Earth Syst. Sci. Data *14*, 1917–2005. https://doi.org/10.5194/essd-14-1917-2022.

37. O'Neill, B.C., Tebaldi, C., Van Vuuren, D.P., Eyring, V., Friedlingstein, P., Hurtt, G., Knutti, R., Kriegler, E., Lamarque, J.-F., Lowe, J., et al. (2016). The Scenario Model Intercomparison Project (ScenarioMIP) for CMIP6. Geosci. Model Dev. *9*, 3461–3482. https://doi.org/10.5194/gmd-9-3461-2016.

38. Meinshausen, M., Nicholls, Z.R.J., Lewis, J., Gidden, M.J., Vogel, E., Freund, M., Beyerle, U., Gessner, C., Nauels, A., Bauer, N., et al. (2020). The shared socio-economic pathway (SSP) greenhouse gas concentrations and their extensions to 2500. Geosci. Model Dev. *13*, 3571–3605. https://doi.org/10.5194/gmd-13-3571-2020.

39. Huppmann, D., Kriegler, E., Krey, V., Riahi, K., Rogelj, J., Rose, S.K., Weyant, J., Bauer, N., Bertram, C., Bosetti, V., et al. (2018). IAMC 1.5°C Scenario Explorer and Data Hosted by IIASA (Integrated Assessment Modeling Consortium & International Institute for Applied Systems Analysis). https://doi.org/10.22022/SR15/08-2018.15429.

40. Rogelj, J., Shindell, D., Jiang, K., Fifita, S., Forster, P., Ginzburg, V., Handa, C., Kheshgi, H., Kobayashi, S., Kriegler, E., et al. (2018). Mitigation pathways compatible with 1.5°C in the context of sustainable development. In Special Report on the impacts of global warming of 1.5°C (Intergovernmental Panel on Climate Change).

41. Xu, J., Morris, P.J., Liu, J., and Holden, J. (2018). PEATMAP: Refining estimates of global peatland distribution based on a meta-analysis. Catena *160*, 134–140. https://doi.org/10.1016/j.catena.2017.09.010.

42. Tuomi, M., Vanhala, P., Karhu, K., Fritze, H., and Liski, J. (2008). Heterotrophic soil respiration—Comparison of different models describing its temperature dependence. Ecol. Model. *211*, 182–190. https://doi.org/10.1016/j.ecolmodel.2007.09.003.

43. Gasser, T., Kechiar, M., Ciais, P., Burke, E.J., Kleinen, T., Zhu, D., Huang, Y., Ekici, A., and Obersteiner, M. (2018). Path-dependent reductions in CO2 emission budgets caused by permafrost carbon release. Nat. Geosci. *11*, 830–835. https://doi.org/10.1038/s41561-018-0227-0.

44. Lange, S., and Büchner, M. (2022). Secondary ISIMIP3b bias-adjusted atmospheric climate input data. Version 1.1 (ISIMIP Repository). https://doi.org/10.48364/ISIMIP.581124.1.

45. Zhang, Y., Goll, D., Bastos, A., Balkanski, Y., Boucher, O., Cescatti, A., Collier, M., Gasser, T., Ghattas, J., Li, L., et al. (2019). Increased Global Land Carbon Sink Due to Aerosol-Induced Cooling. Glob. Biogeochem. Cycles *33*, 439–457. https://doi.org/10.1029/2018GB006051.